Published by Institute of Physics Publishing for SISSA/ISAS
Received: *April 24, 2003*
Accepted: *May 17, 2003*

Time dependent solution in cubic string field theory

Masako Fujita and Hiroyuki Hata

Department of Physics, Kyoto University
Kyoto 606-8502, Japan
E-mail: masako@gauge.scphys.kyoto-u.ac.jp, hata@gauge.scphys.kyoto-u.ac.jp

Abstract: We study time dependent solutions in cubic open string field theory which are expected to describe the configuration of the rolling tachyon. We consider the truncated system consisting of component fields of level zero and two, which are expanded in terms of $\cosh nx^0$ modes. For studying the large time behavior of the solution we need to know the coefficients of all and, in particular, large n modes. We examine numerically the coefficients of the n-th mode, and find that it has the leading n-dependence of the form $(-\beta)^n \lambda^{-n^2}$ multiplied by a peculiar subleading part with peaks at $n = 2^m = 4, 8, 16, 32, 64, 128, \ldots$. This behavior is also reproduced analytically by solving simplified equations of motion of the tachyon system.

Keywords: Bosonic Strings, Tachyon Condensation, String Field Theory.

Contents

1. Introduction **1**

2. CSFT action and the equation of motion **3**

3. Numerical analysis **4**
- 3.1 Numerical analysis for tachyon field 5
- 3.2 Inclusion of level 2 fields 8

4. Analytical consideration **9**

5. Summary and discussions **13**

A. g_n for specific values of n **15**

1. Introduction

Recently the time dependent decay of an unstable D-brane has been one of the most active subjects in string theory. The unstable D-brane evolves in time as the tachyon field rolls down to the bottom of the potential corresponding to the stable closed string vacuum. Sen proposed a boundary conformal field theory (BCFT) which describes this time dependent process [1]. This BCFT is exactly solvable [2, 3, 4] and he found that in the limit of vanishing string coupling the system evolves to a pressureless gas called tachyon matter [5]. Since tachyon matter is classically stable, it could be applied to cosmology as inflaton, and the tachyon matter cosmology has attracted great interest.

Besides such cosmological applications, time dependent solutions themselves are of importance in string theory. For they are expected to reveal new nonperturbative aspects of string dynamics. Much work has been done for the study of the rolling tachyon solutions using various formulations such as conformal field theory, effective field theory, boundary string field theory, supergravity, and so on [6]–[17]. However, there are many problems left unresolved. For example, closed string emission and its back reaction in the process of rolling [6, 16, 17].

In this paper, we study time dependent solutions describing the rolling tachyon in cubic string field theory (CSFT) [18]. We construct time dependent solutions in truncated CSFT and examine whether the solutions have the properties of the rolling tachyon. The

JHEP05(2003)043

desirable properties are as follows:

1. There is a one-parameter family of solutions. This parameter β corresponds to the initial value of tachyon field.

2. For $\beta = 0$, the tachyon stays at the unstable perturbative vacuum:

$$t(x; \beta = 0) = 0 \,. \tag{1.1}$$

3. There is a specific value β_c of β. At $\beta = \beta_c$ the tachyon field is independent of time and stays at the tachyon vacuum:

$$t\left(x^0; \beta_c\right) = t_c \,. \tag{1.2}$$

4. For $0 < \beta < \beta_c$, the tachyon evolves in time and asymptotically approaches the tachyon vacuum t_c:

$$t(x \to \infty; \beta \neq 0) = t_c \,. \tag{1.3}$$

We expand the component fields in terms of $\cosh nx^0$ (and $\sinh nx^0$) and solve the equations of motion for the modes [19, 20]. For example, in the truncated system of only the level zero tachyon field $t(x^0)$, we express it as

$$t\left(x^0\right) = \sum_{n=0}^{\infty} t_n \cosh nx^0 \,, \tag{1.4}$$

and solve the equations of motion for t_n $(n \neq 1)$ by taking t_1 as a given parameter corresponding to the marginal deformation parameter in the full CSFT system.[1] However, if we truncate the summation in (1.4) at $n = N$ as in the modified level truncation scheme [23], the solution diverges like $\cosh Nx^0$ as $x^0 \to \infty$. A hint on avoiding this divergent behavior is found in the calculation of the coefficient $f(x^0)$ of the closed string tachyon in the rolling tachyon boundary state [1]. There, an infinite summation of $\cosh nx^0$ gives a finite value at $x^0 \to \infty$ by analytic continuation:

$$f\left(x^0\right) = 1 + 2\sum_{n=1}^{\infty} \left(-\widetilde{\beta}\right)^n \cosh nx^0 = \frac{1}{1+\widetilde{\beta}\, e^{x^0}} + \frac{1}{1+\widetilde{\beta}\, e^{-x^0}} - 1 \,. \tag{1.5}$$

Moreover, at a specific value of the parameter $\widetilde{\beta}$; $\widetilde{\beta} = 1$, the summation becomes a constant, which is a desirable property for the rolling tachyon solution. This example suggests that, for getting a convergent function at $x^0 \to \infty$, we have to obtain the coefficients t_n for all, and in particular, large n and carry out the infinite summation of (1.4).

In this paper, we first solve numerically the equation of motion of t_n to study its n-dependence. We find that t_n has a leading n-dependence of the form $(-\beta)^n \lambda^{-n^2}$ with β being proportional to the parameter t_1. Besides this leading n-dependence, t_n has a

[1] See [20, 21, 22] for approaches to solving the differential equations of the component fields without using the mode expansion.

peculiar subleading part with peaks at $n = 2^m = 4, 8, 16, 32, 64, 128, \ldots$. Then we carry out analytical study of the equation of motion of t_n. Since the original equation of motion is too complicated to be solved analytically, we consider an approximate equation of motion valid for a large n. This equation is further deformed to a simplified one which still maintains the essential features of the original equation. In fact, this simplified equation can be solved analytically at special values of n to reproduce the behavior of t_n found by numerical analysis.

The rest of this paper is organized as follows. In section 2, we present the CSFT action and the equation of motion of t_n. In section 3, we carry out the numerical analysis of t_n and also the level two modes, and find their n-dependence. Then in section 4, the equation of motion of t_n is examined analytically to reproduce their n-dependence found in section 3. The final section (section 5) is devoted to a summary and discussions. In the appendix, we present technical details used in section 4.

2. CSFT action and the equation of motion

The action of cubic string field theory for bosonic open string takes the form [18]

$$S = -\frac{1}{g_0^2}\left(\frac{1}{2}\Phi \cdot Q_{\mathrm{B}}\Phi + \frac{1}{3}\Phi \cdot (\Phi * \Phi)\right), \tag{2.1}$$

where Q_{B} is the BRST operator and $*$ is the star product between two string fields. The open string field Φ contains component fields corresponding to all the states in the first-quantized string Fock space. For more details of CSFT and its application to tachyon condensation, see [24] and the references therein. First let us keep only the tachyon field $t(x)$ in Φ, $|\Phi\rangle = b_0|0\rangle t(x)$. The truncated action including only the tachyon field is

$$S = \frac{1}{g_0^2}\int d^{26}x\left(\frac{1}{2}t(x)\left(\Box + 1\right)t(x) - \frac{1}{3}\lambda\left(\lambda^{(1/3)\Box}t(x)\right)^3\right), \tag{2.2}$$

with

$$\Box = -\partial_0^2 + \nabla^2, \qquad \lambda = \frac{3^{9/2}}{2^6} = 2.192\,. \tag{2.3}$$

We use the convention of $\alpha' = 1$ throughout this paper. Later we shall take into account of the level two fields.

In the following we are interested in the time dependent and spatially homogeneous solution $t(x^0)$ to the equation of motion derived from (2.2):

$$\left(\partial_0^2 - 1\right)t\left(x^0\right) + \lambda^{1-\partial_0^2/3}\left(\lambda^{-\partial_0^2/3}t\left(x^0\right)\right)^2 = 0\,. \tag{2.4}$$

As we mentioned in section 1, we expand the tachyon field in terms of $\cosh nx^0$ following [20, 19]. Here, we do not adopt the modified level truncation scheme [23], but take into account of all the modes:

$$t\left(x^0\right) = \sum_{n=0}^{\infty} t_n \cosh nx^0\,. \tag{2.5}$$

Substituting this into the equation of motion (2.4), we have the following equations for each t_n:

$$-t_0+\lambda\left[(t_0)^2+\frac{1}{2}\sum_{n=1}^{\infty}\lambda^{-2n^2/3}\,(t_n)^2\right]=0\,, \tag{2.6}$$

$$2\,t_0\,t_1+\sum_{k=1}^{\infty}\lambda^{-2k(k+1)/3}\,t_k\,t_{k+1}=0\,, \tag{2.7}$$

$$\begin{aligned}(n^2-1)\,t_n+\lambda^{1-2n^2/3}\Bigg[2\,t_0\,t_n+\frac{1}{2}\sum_{k=1}^{n-1}\lambda^{-2k(k-n)/3}\,t_k\,t_{n-k}+\\ +\sum_{k=1}^{\infty}\lambda^{-2k(k+n)/3}\,t_k\,t_{n+k}\Bigg]=0\quad(n\geq 2)\,,\end{aligned} \tag{2.8}$$

which are respectively the equations of motion of t_0, t_1 and t_n $(n\geq 2)$.

From the BCFT analysis of rolling tachyon [1], it is expected that the full CSFT keeping all the component fields in Φ has a rolling solution with one free parameter corresponding to the initial value of the tachyon field at $x^0=0$. However, in the approximate analysis with finite number of component fields, we no longer have such a free parameter. Therefore, in our analysis we treat t_1 as a given parameter and solve (2.6) and (2.8) for $t_n(t_1)$ $(n=0,2,3,\dots)$ [20, 19]. In the exact CSFT, we can in principle adopt any t_n as the free parameter. However, in our approximate analysis the result depends on choice of the free parameter. The present choice is natural since, in the case without the interaction in (2.4), the solution is given by $t_1\cosh x^0$ with t_1 being arbitrary.

Before starting the numerical analysis of $t_n(t_1)$, we shall mention that the parameter t_1 has an upper bound t_1^{c} above which (2.6) and (2.8) have no real solutions [19]. To understand this fact it is sufficient to consider only t_0 neglecting other t_n with $n\geq 2$, since they are negligibly small compared with t_0 as we shall see in later sections. Solving (2.6) with $t_n=0$ $(n\geq 2)$, we have two branches of solutions [19],

$$t_0^{(\pm)}(t_1)=\frac{1}{2\lambda}\left(1\pm\sqrt{1-\left(\frac{t_1}{t_1^{\mathrm{c}}}\right)^2}\right)\,, \tag{2.9}$$

with t_1^{c} given by

$$t_1^{\mathrm{c}}=\frac{1}{\sqrt{2}}\,\lambda^{-2/3}=0.419\,. \tag{2.10}$$

The solutions $t_0^{(+)}$ and $t_0^{(-)}$ are those connected with the tachyon vacuum $t(x)=1/\lambda$ and the unstable perturbative vacuum $t(x)=0$, respectively, and $t_0^{(-)}$ is the rolling solution we are interested in. Both $t_0^{(\pm)}$ are real only in the region $|t_1|\leq t_1^{\mathrm{c}}$.

3. Numerical analysis

In this section we shall carry out numerical analysis of the rolling solutions in CSFT. In section 3.1, we solve numerically the equation of motion of only the level zero tachyon field $t(x^0)$. Then in section 3.2 we extend our analysis to the system with level two fields.

3.1 Numerical analysis for tachyon field

As we mentioned in the previous section, we solve numerically the equations of motion (2.6) and (2.8) for t_0 and t_n $(n \geq 2)$ for a given value of t_1. Since numerical calculation cannot be done for an infinite number of variables t_n, we put $t_n \equiv 0$ for $n > N$ with sufficiently large N and solve (2.6) and (2.8) for $n \leq N$. Here, we take $N = 150$ and obtain the solution t_n $(n = 0, 2, 3, \ldots, 150)$ by Newton's method starting with the point $t_n = 0$ (namely, we are considering the solution which is reduced to the perturbative vacuum in the limit $t_1 \to 0$). We have obtained $t_n(t_1)$ at discrete points $t_1 = 0.01, 0.02, 0.03, \ldots, 0.41$ and 0.418. There exists no real solutions for $t_1 \gtrsim 0.419$, which is consistent with the simplified analysis of (2.9). Figure 1 shows $-\ln|t_n|$ $(n \geq 2)$ at $t_1 = 0.1$.

Then, let us assume that the n-dependence of t_n at each value of t_1 is given by

$$t_n^{\rm fit} = -A\,\lambda^{-\xi n^2}(-\beta)^n\,, \qquad (n \geq 2)\,, \tag{3.1}$$

and obtain $A(t_1)$, $\xi(t_1)$ and $\beta(t_1)$ by fitting to our numerical solution $t_n(t_1)$. This assumption of (3.1) will be justified by analytical considerations in the next section. The solution t_n and the fitted curve (3.1) at, for example, $t_1 = 0.1$ are shown in figure 2, which confirms the validity of our assumption (3.1). Fitting by (3.1) works very well also at other values of t_1. Figures 3, 4 and 5 show $\xi(t_1)$, $\beta(t_1)$ and $A(t_1)$ obtained by fitting. These results show that

$$\xi(t_1) \simeq 1\,, \tag{3.2}$$

$$\beta(t_1) \propto t_1\,(\simeq 0.196\,t_1)\,, \tag{3.3}$$

and that $A(t_1)$ is almost a constant. Figure 3 (with $N = 150$) itself tells that $\xi \simeq 1.00026$ with little t_1-dependence. For other values of the cutoff N, we have $\xi \simeq 1.0045$ $(N = 50)$ and $\xi \simeq 1.00148$ $(N = 100)$. These results strongly suggest that $\xi(t_1)$ approaches a constant which is equal to one in the limit $N \to \infty$. As for $\beta(t_1)$, the proportionality constant (0.196 for $N = 150$) for other values of N are 0.2391 $(N = 50)$ and 0.2137 $(N = 100)$. The proportionality constant gradually decreases as N becomes larger, and the value at $N = \infty$

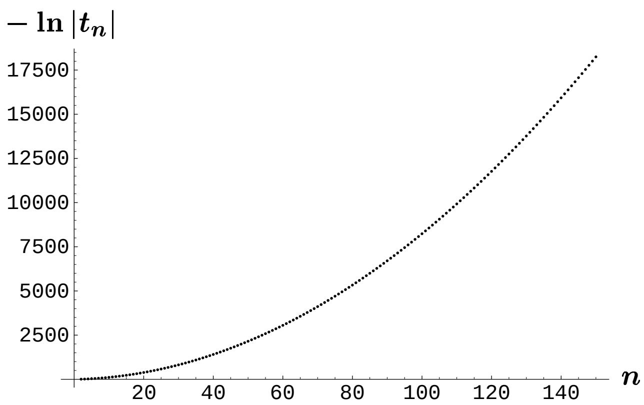

Figure 1: $-\ln|t_n|$ for $n = 2, 3, \ldots, 150$ at $t_1 = 0.1$.

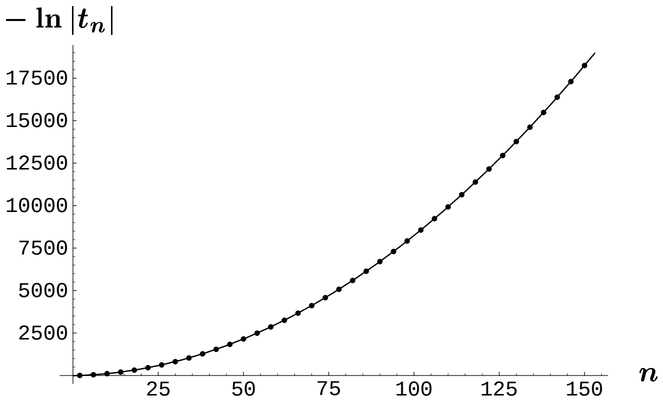

Figure 2: The numerical solution $-\ln|t_n|$ (dots) and the fitted curve $0.7851\,n^2 + 3.929\,n - 6.620$, which corresponds to $\xi = 1.00024$, $\beta = 0.01986$ and $A = 749.6$. For the sake of visibility, the dots representing the numerical solution are plotted only for $n = 2, 6, 10, 14, \ldots, 150$.

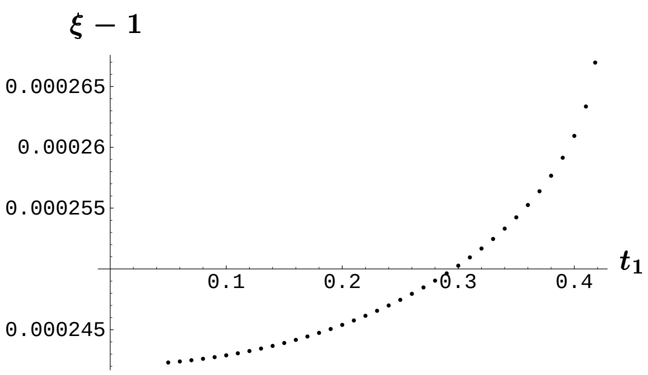

Figure 3: $\xi(t_1) - 1$ at $t_1 = 0.05, 0.06, \ldots, 0.41$ and 0.418. The dots representing $\xi(t_1)$ for $t_1 \leq 0.04$ are missing since t_n with larger n vanishes in our numerical precision, which makes it impossible to determine ξ by fitting.

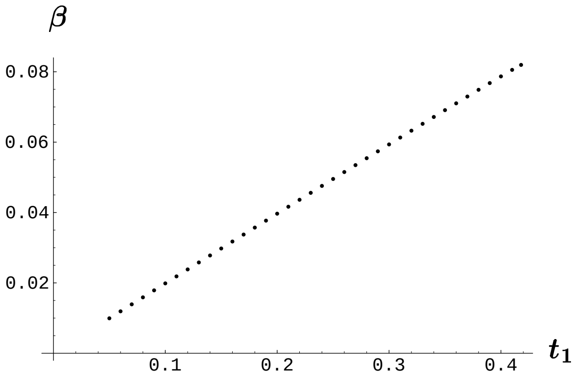

Figure 4: $\beta(t_1)$ at $t_1 = 0.05, 0.06, \ldots, 0.41$ and 0.418. For the same reason as in the case of $\xi(t_1)$ (figure 3), the dots are missing for $t_1 \leq 0.04$.

predicted by the fitting using $a + b/N$ is 0.18. The value of β at $t_1 = 0.418$ which is close to the critical t_1 above which we have no real solutions is $\beta(0.418) = 0.0819$ for $N = 150$. For other values of N, we have $\beta(0.418) = 0.0999$ $(N = 50)$ and $\beta(0.418) = 0.0893$ $(N = 100)$.

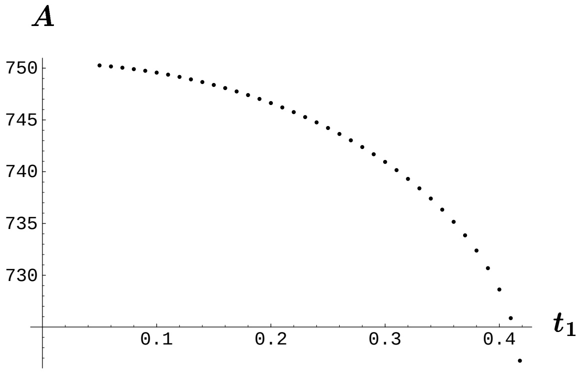

Figure 5: $A(t_1)$ at $t_1 = 0.05, 0.06, \ldots, 0.41$ and 0.418. For the same reason as in the case of $\xi(t_1)$ (figure 3), the dots are missing for $t_1 \leq 0.04$.

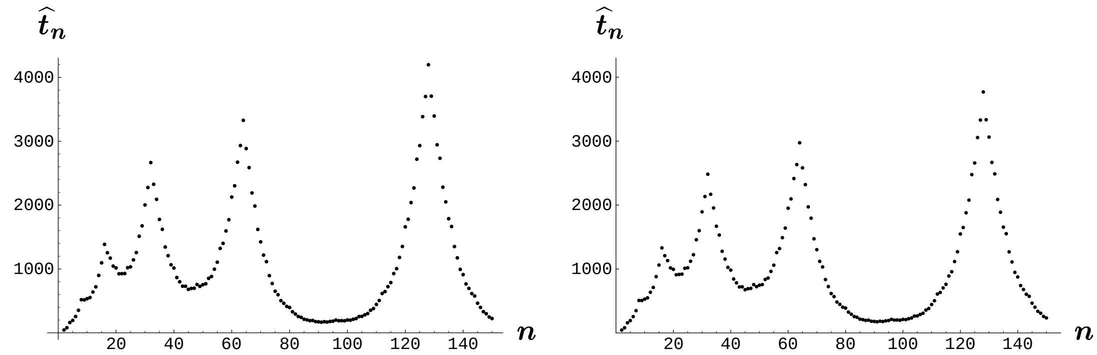

Figure 6: $\widehat{t}_n$ at $t_1 = 0.1$ (left figure) and $t_1 = 0.4$ (right figure). There are peaks at $n = 4, 8, 16, 32, 64, 128$. The shapes of these two figures are almost the same.

Then let us consider the deviation of t_n from the leading n-dependence (3.1). Figure 6 shows

$$\widehat{t}_n = -\frac{t_n}{\lambda^{-\xi n^2}(-\beta)^n}\,, \tag{3.4}$$

at $t_1 = 0.1$ and 0.4 (ξ and β in the denominator are those given by figures 3 and 4). The coefficient A of (3.1) is the average value of $\widehat{t}_n$ with respect to n. As seen from figure 6, the subleading part $\widehat{t}_n$ has a peculiar n-dependence; it has peaks at $n = 2^m = 4, 8, 16, 32, 64, 128$. In addition, $\widehat{t}_n(t_1)$ depends very little on the value of t_1. These properties of $\widehat{t}_n$ will be partially reproduced by analytical consideration in section 4.

Finally, figure 7 shows the l.h.s. of (2.7) for the present solution $t_n(t_1)$ and the solution obtained by starting from the tachyon vacuum. It shows how well the equation of motion of t_1, which we do not take into account in obtaining the solution, is satisfied. As seen from the figure, the equation of motion of t_1 is fairly well satisfied by the solution connected to the perturbative vacuum. Since t_n with larger n are negligibly small as seen from (3.1), the behavior of (2.7) given by figure 7 is almost the same as that obtained by the simplified analysis using (2.9) and neglecting other t_n.

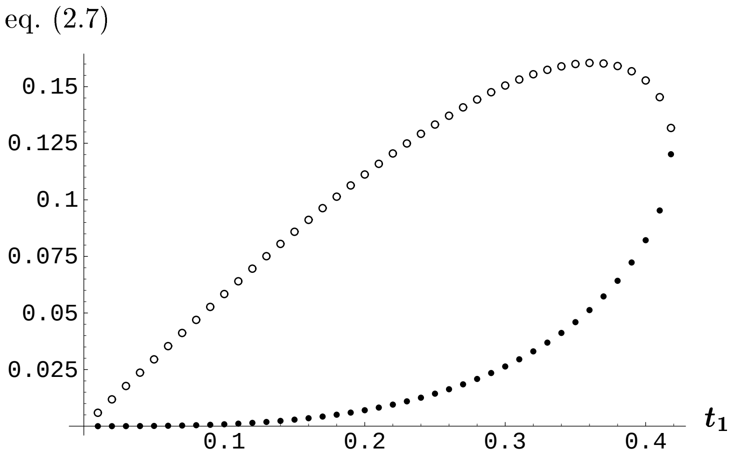

Figure 7: The l.h.s. of (2.7) for the solution $t_n(t_1)$ obtained by starting from the perturbative vacuum (dots) and that from the tachyon vacuum (circles).

3.2 Inclusion of level 2 fields

We have carried out the same kind of analysis as in the previous subsection by including the level two fields. Taking into account of spatial rotational symmetry, twist symmetry and the invariance under $X \to -X$ [23], the string field $|\Phi\rangle = b_0|\phi\rangle$ in the Siegel gauge with component fields up to level two is expanded as follows:

$$|\phi(x^0)\rangle = |0\rangle\, t(x^0) + c_{-1}b_{-1}|0\rangle\, u(x^0) - \frac{1}{2}\left(\alpha^0_{-1}\right)^2|0\rangle\, v(x^0) - \\ -i\,\alpha^0_{-2}|0\rangle\,\chi(x^0) + \frac{1}{2}\alpha^i_{-1}\alpha^i_{-1}|0\rangle\, w(x^0)\,, \tag{3.5}$$

where t, u, v and w are even functions of x^0 and hence are expanded by $\cosh nx^0$; $\varphi(x^0) = \sum_{n=0}^{\infty}\varphi_n \cosh nx^0$ ($\varphi = t,\, u,\, v,\, w$), while χ is an odd function and is expanded by $\sinh nx^0$; $\chi(x^0) = \sum_{n=1}^{\infty}\chi_n \sinh nx^0$. These five fields are all hermitian. We have used the level $(2,6)$ action in our calculation.[2]

In this numerical analysis, we adopted $N = 30$ as the cutoff of the mode number n for all the five fields and solved the equation of motion of each mode for a given value of t_1. Then, fitting the solution $t_n(t_1)$ by (3.1), we obtained $\xi(t_1)$ and $\beta(t_1)$, which are shown in figures 8 and 9.[3] The critical value of t_1 above which there is no real solution is $t_1^{\mathrm{c}} \simeq 0.46$ in the present case, which is larger than that in the purely t system. Figure 8 is consistent

[2]Here, we do not adopt the modified level truncation scheme as in [20], but we assign level zero to t_n and level two to u_n, v_n, χ_n and w_n for all n. The set of component fields in our level $(2,6)$ analysis is not included nor includes that of the modified level $(4,8)$ analysis in [20, section 7]. For the common component fields, the correspondence between [20] (denoted by the superscript MZ) and the present paper is $v_1^{\mathrm{MZ}} = (1/3)\left(2\sqrt{2}\chi_1 - v_1\right)$ and $z_1^{\mathrm{MZ}} = (1/3)\left(v_1 - \chi_1/\sqrt{2}\right)$ (t_0, t_1, u_0, u_1, v_0, w_0 and w_1 are the same between the two). Comparing the numerical solution at $t_1 = 0.05$ given in [20, section 7] with ours, we find that t_0, u_0, v_0, w_0 and t_2 agree within the accuracy of 0.1%, while the agreement is only up to factor for u_1, v_1 and w_1.

[3]In obtaining $\xi(t_1)$ and $\beta(t_1)$ by fitting, we omitted t_5, t_6 and t_{18}. Inclusion of them in the fit leads to $\xi(t_1)$ and $\beta(t_1)$ with strange t_1-dependence since t_5, t_6 and t_{18} change their signs at $t_1 \sim 0.30$, 0.26 and 0.37, respectively.

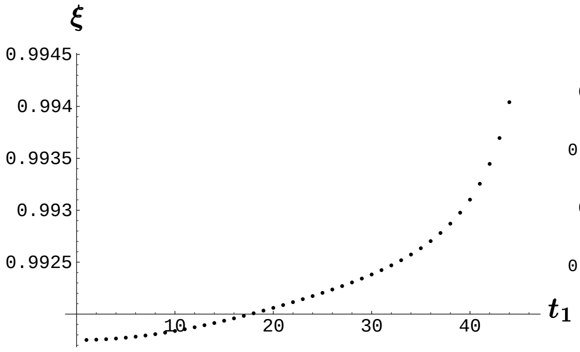

Figure 8: $\xi(t_1)$ at $t_1 = 0.01, 0.02, \ldots, 0.46$ in the level $(2,6)$ analysis.

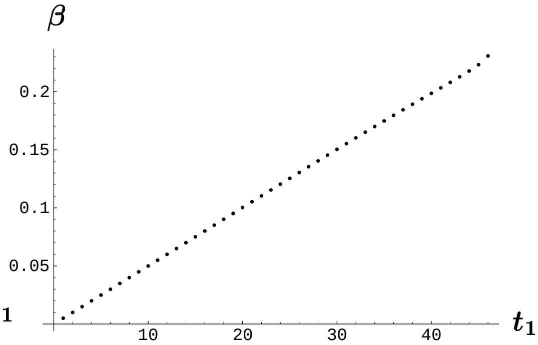

Figure 9: $\beta(t_1)$ at $t_1 = 0.01, 0.02, \ldots, 0.46$ in the level $(2,6)$ analysis. The value of β at $t_1 = 0.46$ is $\beta(0.46) = 0.23$.

with our previous result (3.2), $\xi(t_1) \simeq 1$. From figure 9 we have

$$\beta(t_1) \simeq 0.50\, t_1 \,. \tag{3.6}$$

In particular, the value of β at the critical t_1 is $\beta(t_1 = 0.46) \simeq 0.23$, which is about three times larger than that in the purely t system of section 3.1. The n-dependences of other modes φ_n $(\varphi = u, v, w, \chi)$ are similar to that of t_n.

In our level $(2,6)$ analysis with $N = 30$, the subleading part $\widehat{t}_n$ (3.4) does not show such characteristic behavior as in figure 6. This could be due to that $N = 30$ is not sufficiently large.

4. Analytical consideration

In this section, we would like to understand analytically the n-dependence of t_n found in the previous section, namely, (3.2), (3.3) and the peculiar behavior of the subleading part $\widehat{t}_n$ given by figure 6.

Let us consider the equation of motion (2.8) for large n. We assume that the solution t_n is given by

$$t_n = -(-1)^n \frac{2}{\lambda}\, g_n\, \lambda^{-(2/3)cn^2} \qquad (n \geq 1)\,, \tag{4.1}$$

where c is a constant and g_n has a weaker n-dependence than the leading term $\lambda^{-(2/3)cn^2}$. Concretely, we expect that $\ln g_n = \mathcal{O}(n)$ for $n \gg 1$. The front factor $(-1)^n 2/\lambda$ is simply for the sake of later convenience. Note that, if t_n is a solution, so is $(-1)^n t_n$.

We rewrite (2.8) into

$$\left(n^2 - 1\right) t_n + \lambda^{1-(2/3)n^2} \left(2t_0 t_n + Y_n + Z_n\right) = 0\,, \tag{4.2}$$

where Y_n and Z_n are defined by

$$Y_n = \frac{1}{2} \sum_{k=1}^{n-1} \lambda^{2k(n-k)/3} t_{n-k} t_k \,, \tag{4.3}$$

$$Z_n = \sum_{k=1}^{\infty} \lambda^{-2k(k+n)/3} t_{n+k} t_k \,. \tag{4.4}$$

JHEP05(2003)043

Substituting the ansatz (4.1) to Y_n and Z_n, we obtain

$$Y_n = \frac{2}{\lambda^2}(-1)^n \lambda^{-(2/3)(c/2-1/4)n^2} \sum_{k=1-n/2}^{n/2-1} \lambda^{-(2/3)(1+2c)k^2} g_{\frac{n}{2}-k} g_{\frac{n}{2}+k} , \tag{4.5}$$

$$Z_n = \frac{4}{\lambda^2}(-1)^n \lambda^{-(2/3)(c/2-1/4)n^2} \sum_{k=1+n/2}^{\infty} \lambda^{-(2/3)(1+2c)k^2} g_{\frac{n}{2}+k} g_{-\frac{n}{2}+k} , \tag{4.6}$$

where the summations with respect to k run over integers (half-an-odd integers) when n is even (odd). Since the summation in Y_n is convergent in the limit $n \to \infty$, we have

$$Y_n \sim \lambda^{-(2/3)(c/2-1/4)n^2} , \qquad (n \gg 1) . \tag{4.7}$$

On the other hand, the large n behavior of Z_n is

$$Z_n \sim \lambda^{-(2/3)(c/2-1/4)n^2} \times \lambda^{-(2/3)(1+2c)(1+n/2)^2} \sim \lambda^{-(2/3)cn^2} , \qquad (n \gg 1) . \tag{4.8}$$

Therefore, we have

$$Y_n \gg Z_n \sim t_n , \qquad (n \gg 1) , \tag{4.9}$$

and we can neglect $2t_0t_n$ and Z_n in the second term of (4.2) for a large n. The constant c is determined by the requirement that the first term $(n^2-1)t_n \sim \lambda^{-(2/3)cn^2}$ of (4.2) and the leading part $\lambda^{1-(2/3)n^2} Y_n \sim \lambda^{-(c/3+1/2)n^2}$ of the second term have the same large n behavior:

$$c = \frac{3}{2} . \tag{4.10}$$

Therefore, the equation of motion (4.2) for t_n is reduced to

$$g_n = \frac{1}{n^2-1} \sum_{k=1-n/2}^{n/2-1} \lambda^{-(8/3)k^2} g_{\frac{n}{2}-k} g_{\frac{n}{2}+k} . \tag{4.11}$$

Although (4.11) has been derived for a sufficiently large n, let us assume that it is valid for all $n(\geq 2)$. Then, since the r.h.s. of (4.11) is given in terms of g_k with k smaller than n, (4.11) determines g_n recursively once we fix $g_1 = (\lambda^2/2)t_1$. In fact, numerical analysis shows that (4.11) reproduces the peculiar subleading behavior of figure 6.

For analytic evaluation of g_n, let us make a further simplification on (4.11) which can still reproduce the behavior of t_n observed in section 3. This simplification is to keep only the term with the smallest $|k|$ in the summation of (4.11) by regarding that $\lambda^{-8/3} = 0.12$ is sufficiently small:

$$g_n = \frac{1}{n^2-1} \times \begin{cases} \left(g_{n/2}\right)^2 & (n : \text{even}) \\ \eta \, g_{(n-1)/2} \, g_{(n+1)/2} & (n : \text{odd}) , \end{cases} \tag{4.12}$$

with

$$\eta = 2\lambda^{-2/3} = \frac{32}{27} . \tag{4.13}$$

Eq. (4.12) is still too complicated to be solved analytically for a generic n. However, we can obtain the solution g_n for specific values of n; $n = 2^m + 2^{m-1} + \cdots + 2^{m-a} = 2^m(2-2^{-a})$ $(0 \le a \le m)$ and $n = 2^m + 2^{m-b} = 2^m(1+2^{-b})$ $(0 \le b \le m)$. These n are of the form $11\cdots100\cdots0$ and $10\cdots010\cdots0$ in the binary notation. For $n = 2^m(2-2^{-a})$, (4.12) gives

$$\begin{aligned} g_{2^{m+1}-2^{m-a}} &= \frac{1}{(2^{m+1}-2^{m-a})^2-1}\left(g_{2^m-2^{m-a-1}}\right)^2 \\ &= \prod_{k=0}^{m-a-1}\left(\frac{1}{(2^{m+1-k}-2^{m-a-k})^2-1}\right)^{2^k}\left(g_{2^{a+1}-1}\right)^{2^{m-a}}, \end{aligned} \tag{4.14}$$

which in the special case of $a=0$ is the equation for g_{2^m}. Then, using again (4.12), $g_{2^{a+1}-1}$ on the r.h.s. of (4.14) is given as

$$g_{2^{a+1}-1} = \frac{\eta}{(2^{a+1}-1)^2-1}g_{2^a}g_{2^a-1} = \prod_{k=0}^{a-1}\frac{\eta}{(2^{a-k+1}-1)^2-1}\prod_{\ell=0}^{a}g_{2^{a-\ell}}\,, \tag{4.15}$$

and the final factor $g_{2^{a-\ell}}$ in (4.15) is expressed in terms of g_1 using (4.14) with $a=0$ and $m = a-\ell$. Completing the calculations we obtain $g_{n=2^m(2-2^{-a})}$ in a closed form as a function of g_1 (see appendix A). In particular, for a large $n = 2^m(2-2^{-a})$ we have

$$g_{n=2^m(2-2^{-a})} = 16\left(\frac{g_1}{G_a}\right)^n\left(n^2-\frac{1}{7}+\mathcal{O}\left(n^{-2}\right)\right). \tag{4.16}$$

In (4.16), G_a depends on only a and is given by

$$G_a = \left(\frac{2^{(a^2+5a+8)/2}}{\eta^a}T_a^2\,e^{-S_a}\prod_{k=1}^{a}\left(2^k-1\right)\cdot\prod_{p=0}^{a-1}\prod_{q=0}^{a-p-1}\left(2^{2(a-p-q)}-1\right)^{2^q}\right)^{1/T_a}, \tag{4.17}$$

where T_a and S_a are defined by

$$T_a = 2^{a+1}-1\,, \tag{4.18}$$

$$S_a = \sum_{p=1}^{\infty}\frac{\left(2^{a+1}-1\right)^{-2p}}{p\left(2^{2p+1}-1\right)}. \tag{4.19}$$

Similarly, for $n = 2^m(1+2^{-b})$ we have

$$g_{n=2^m(1+2^{-b})} = 16\left(\frac{g_1}{\widetilde{G}_b}\right)^n\left(n^2-\frac{1}{7}+\mathcal{O}\left(n^{-2}\right)\right), \tag{4.20}$$

where $\widetilde{G}_b$ is given by

$$\widetilde{G}_b = \left(\frac{3\cdot 2^{(b^2+3b+8)/2}}{\eta^b}\widetilde{T}_b^2 e^{-\widetilde{S}_b}\prod_{k=0}^{b-1}(2^k+1)\cdot\prod_{p=0}^{b-2}\prod_{q=0}^{b-p-2}\left(2^{2(b-p-q-1)}-1\right)^{2^q}\right)^{1/\widetilde{T}_b}, \tag{4.21}$$

with

$$\widetilde{T}_b = 2^b+1\,, \tag{4.22}$$

$$\widetilde{S}_b = \sum_{p=1}^{\infty}\frac{\left(2^b+1\right)^{-2p}}{p\left(2^{2p+1}-1\right)}. \tag{4.23}$$

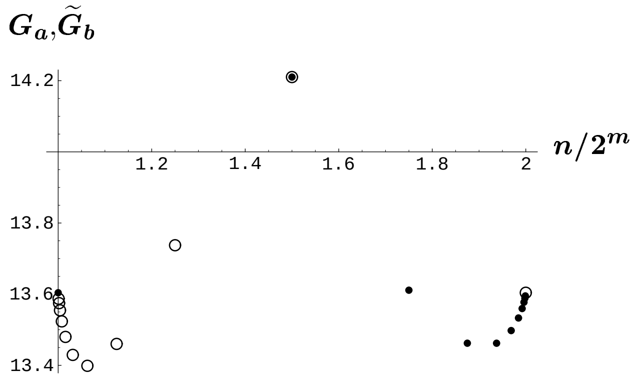

Figure 10: G_a (dots) and $\widetilde{G}_b$ (circles). The horizontal axis is $n/2^m = 2 - 2^{-a}$ for G_a and $n/2^m = 1 + 2^{-b}$ for $\widetilde{G}_b$. Here we use the original value $\eta = 2\lambda^{-2/3} = 32/27$.

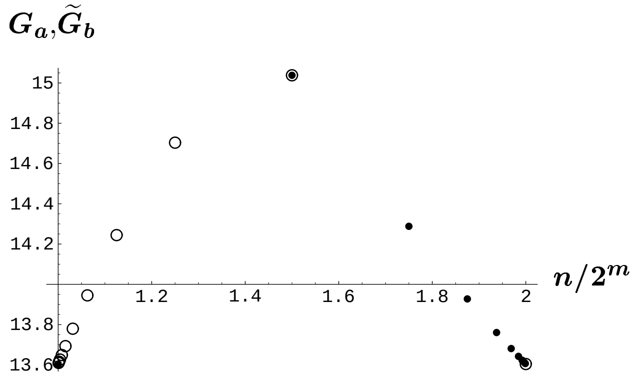

Figure 11: G_a (dots) and $\widetilde{G}_b$ (circles) as functions of $n/2^m$ calculated by adopting $\eta = 1$.

In (4.17) and (4.21), the products $\prod_{k=n}^{m}$ with $n > m$ are defined to be equal to one. For example, the products in (4.17) are missing for G_0.

Let us see the behaviors of G_a and $\widetilde{G}_b$. First, we have

$$G_0 = G_\infty = \widetilde{G}_0 = \widetilde{G}_\infty = 16\, e^{-S_0} = 13.604\,. \tag{4.24}$$

The equality of these four quantities is natural since $a = 0$, $a = \infty$, $b = 0$ and $b = \infty$ all correspond to the points of the same type $n = 2^m$. The value $16\, e^{-S_0}$ is independent of η. Next, figures 10 and 11 show G_a (dots) and $\widetilde{G}_b$ (circles). The horizontal axis is $2 - 2^{-a}$ for G_a and $1 + 2^{-b}$ for $\widetilde{G}_b$ (recall that $n = 2^m(2 - 2^{-a})$ for G_a, and $n = 2^m(1 + 2^{-b})$ for $\widetilde{G}_b$). Since $a = 1$ and $b = 1$ correspond to the same $n = 2^m + 2^{m-1}$, we have $G_1 = \widetilde{G}_1$. The difference between figures 10 and 11 is that we have used the original value $\eta = 32/27$ of (4.13) in the former, while the smaller value $\eta = 1$ has been adopted in the latter (see below for the reason why we consider η different from (4.13)).

Substituting (4.16) and $g_1 = (\lambda^2/2)t_1$ into (4.1), we get for $n \gg 1$

$$t_{n=2^m(2-2^{-a})} = -\frac{32}{\lambda}\left(-\frac{\lambda^2}{2G_a}\,t_1\right)^n \lambda^{-n^2}\left(n^2 - \frac{1}{7} + \mathcal{O}\left(n^{-2}\right)\right). \tag{4.25}$$

Similarly from (4.20), we obtain $t_{n=2^m(1+2^{-b})}$, which is given by (4.25) with G_a replaced by $\widetilde{G}_b$. Let us compare this expression of t_n with the results of our numerical analysis of section 3.1. There t_n was given as (we have put $\xi = 1$)

$$t_n = -\widehat{t}_n \, (-\beta)^n \, \lambda^{-n^2} \, . \tag{4.26}$$

In section 3.1, we first determined β (and ξ) by fitting t_n using (4.26) with $\widehat{t}_n$ treated as n-independent quantity A. We found that the subleading part $\widehat{t}_n$ has a peculiar n-dependence of figure 6. The correspondence between (4.25) and (4.26) should be as follows:

$$\beta(t_1) = \frac{\lambda^2}{2\overline{G}} \, t_1 \, , \tag{4.27}$$

$$\widehat{t}_n = \frac{32}{\lambda} \left(n^2 - \frac{1}{7} + \mathcal{O}(n^{-2}) \right) \left(\frac{\overline{G}}{G_a} \right)^n , \tag{4.28}$$

where $\overline{G}$ is the "average value" of G_a. Here we can treat only the special points of the form $n = 2^m(2 - 2^{-a})$ and $2^m(1 + 2^{-b})$. However, $\overline{G}$ should be regarded as an average of G_a and $\widetilde{G}_b$ over all n points assuming that the formula like (4.25) holds for a generic n.

Let us consider $\beta(t_1)$ of (4.27). If we take $\overline{G} = 14$, which is a reasonable value as seen from figure 10, we have $\lambda^2/(2\overline{G}) = 0.17$. This is close to the proportionality constant of $\beta(t_1)$ determined numerically in section 3.1 (see below (3.3)).

Eq. (4.28) cannot reproduce the peak behavior of figure 6 if we adopt as η the original value (4.13), since G_a and $\widetilde{G}_b$ has minima at points a little off the points $n = 2^m$ as seen from figure 10. However, if we take a smaller value $\eta = 1$ as in figure 11, (4.28) does reproduce the desired peaks at $n = 2^m$ since, in particular, G_a and $\widetilde{G}_b$ take the smallest value at these points. The critical value of η below which G_a and $\widetilde{G}_b$ have minimum at $n = 2^m$ is 1.036. One would think that adopting η different from the original value (4.13) is groundless. However, there is no reason to stick to the original value (4.13) in solving (4.12) since we have made two steps of approximations (the first is the large n approximation and the second is that of $\lambda^{-8/3} \ll 1$) in reaching (4.12) from the original equation of motion. It is expected that, by incorporating the effects in making the approximations, the "effective value" of η in (4.12) is reduced from the original one.

5. Summary and discussions

In this paper, we studied time dependent and spatially homogeneous solutions of the truncated version of cubic string field theory. We expanded the component fields in terms of $\cosh nx^0$ modes, wrote down the equations of motion of the modes, and solved them both numerically and analytically. Our finding in this paper is that the tachyon modes have the leading n-dependence of (3.1) multiplied by the subleading dependence with peaks at $n = 2^m = 4, 8, 16, 32, 64, 128, \ldots$.

Let us return to the question posed in section 1: what the tachyon profile would be if we carry out summations over all modes. First, assuming that t_n is simply given by its

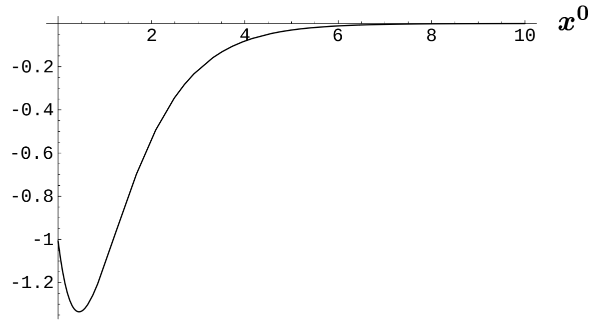

Figure 12: $-\sum_{n=1}^{\infty} \lambda^{-n^2}(-1)^n\,(\beta^n - \beta^{-n})\,e^{-nx}$ at $\beta = 0.1$.

leading part (3.1) with $\xi = 1$ for all $n(\geq 1)$, the profile $t(x^0)$ is given by

$$t(x^0) = t_0 - A\sum_{n=1}^{\infty} \lambda^{-n^2}(-\beta)^n \cosh nx^0\,. \tag{5.1}$$

Unfortunately, this function does not have a desirable behavior as a rolling tachyon solution. It is an oscillating function of x^0 which grows like $\exp\big((x^0)^2/(4\ln\lambda)\big)$ for large x^0.[4]

The function (5.1), however, has other apparently equivalent expressions. Rewriting λ^{-n^2} in (5.1) into $\lambda^{-\partial_0^2}$ and moving it outside the summations, we obtain the second expression:

$$t(x^0) = t_0 + A - \frac{A}{2}\lambda^{-\partial_0^2}\left(\frac{1}{1+\beta\,e^{x^0}} + \frac{1}{1+\beta\,e^{-x^0}}\right), \tag{5.2}$$

with $\lambda^{-\partial_0^2}$ defined by $\lim_{M\to\infty}\sum_{k=0}^{M}(-\ln\lambda)^k/k!\cdot\partial_0^{2k}$. However, the limit $M\to\infty$ does not seem to exist since, as M becomes larger, (5.2) becomes rapidly oscillating with growing amplitude for intermediate values $x^0 \sim \ln(1/\beta)$.

The third definition of $t(x^0)$ is obtained by reexpanding the quantity in the parenthesis of (5.2) in terms of the power series of e^{-x^0} and then moving $\lambda^{-\partial_0^2}$ inside the series:

$$t(x^0) = t_0 + \frac{A}{2} - \frac{A}{2}\sum_{n=1}^{\infty}\lambda^{-n^2}(-1)^n\left(\beta^n - \beta^{-n}\right)e^{-nx^0}. \tag{5.3}$$

This function has a convergent limit as $x^0 \to \infty$. However, it is not a monotonic function of x^0, and what is worse, its derivative at $x^0 = 0$ is not equal to zero in spite of the fact that we started with $\cosh nx^0$ modes (see figure 12).

The origin of the phenomenon that apparently equivalent expressions of $t(x^0)$ give completely different functions is the fact that the insertion of λ^{-n^2} makes any series with finite radius of convergence into another series with infinite radius of convergence. This

[4]This is seen from the formula

$$\sum_{n=-\infty}^{\infty}(-1)^n e^{-an^2-b|n|}\,e^{nx} = e^{x^2/(4a)}\sum_{m=-\infty}^{\infty}\left(e^{-2|m|b}\,e^{-(x-4ma)^2/(4a)} - e^{-|2m-1|b}\,e^{-(x-2(2m-1)a)^2/(4a)}\right)$$

with a and b identified with $\ln\lambda$ and $\ln(1/\beta)$, respectively.

problem is related to the long standing problem of how to treat the infinite derivative operators like $\lambda^{-\partial_0^2}$ in string field theories [25, 26].

The above argument shows that the leading part (3.1) alone cannot give desirable tachyon profiles. Inclusion of the subleading part $\widehat{t}_n$ (3.4) could lead to $t(x^0)$ with a desirable profile. For studying this possibility, we have to solve the equation of motion to obtain analytically the subleading part $\widehat{t}_n$ for all n and carry out the summation over n. However, it is very likely that the problem of $\lambda^{-\partial_0^2}$ persists even if we take into account the subleading part. Another possible way of getting a desirable tachyon profile would be to claim that the tachyon profile should be given by $T(x^0) \equiv \lambda^{\partial_0^2} t(x^0)$ rather than $t(x^0)$ itself: this new $T(x)$ is equal to $t(x)$ in the translationally invariant case, and it gives a monotonic and convergent profile for $t(x^0)$ of (5.2). Besides the tachyon profile itself, we have to study the time dependence of other physical quantities such as the energy-momentum tensor [20, 27].

In this paper we have studied time-dependent solutions in truncated CSFT. It is interesting to construct time-dependent exact solutions of the full CSFT [28]. The tachyon vacuum solution of [29] would be a staring point of the construction. Study of time dependent solutions in vacuum string field theory [30, 31, 32] is also an interesting research subject.

Acknowledgments

We would like to thank S. Sugimoto, T. Takahashi and I. Kishimoto for valuable discussions. The work of H. H. was supported in part by a Grant-in-Aid for Scientific Research from Ministry of Education, Culture, Sports, Science, and Technology (#12640264).

A. g_n for specific values of n

In this appendix we complete solving (4.12) for g_n at $n = 2^m(2-2^{-a})$ and deriving the expression (4.16). The derivation of g_n at $n = 2^m(1+2^{-b})$ is quite similar.

For $g_{n=2^m(2-2^{-a})}$ we have (4.14), (4.15) and

$$g_{2^{a-\ell}} = \prod_{k=0}^{a-\ell-1} \left[\frac{1}{(2^{a-\ell-k})^2-1}\right]^{2^k} (g_1)^{2^{a-\ell}} . \tag{A.1}$$

Substituting (4.15) and (A.1) into (4.14) we obtain a closed expression for $g_{n=2^m(2-2^{-a})}$:

$$g_{n=2^m(2-2^{-a})} = \prod_{k=0}^{m-a-1} \left(\frac{1}{(2^{m+1-k}-2^{m-a-k})^2-1}\right)^{2^k} \cdot \left(\prod_{q=0}^{a-1} \frac{\eta}{(2^{a-q+1}-1)^2-1}\right)^{2^{m-a}} \times$$
$$\times \left(\prod_{\ell=0}^{a}\prod_{p=0}^{a-\ell-1}\left[\frac{1}{(2^{a-\ell-p})^2-1}\right]^{2^p}\right)^{2^{m-a}} (g_1)^n , \tag{A.2}$$

which is valid for any m and a ($0 \leq a \leq m$). For obtaining the approximate expression (4.16), we rewrite the first product in (A.2) into

$$\prod_{k=0}^{m-a-1} \left(\frac{1}{(2^{m+1-k} - 2^{m-a-k})^2 - 1} \right)^{2^k} = \prod_{k=0}^{m-a-1} \left(n^2 \, 2^{-2k} \right)^{-2^k} \prod_{\ell=0}^{m-a-1} \left(1 - n^{-2} 2^{2\ell} \right)^{-2^\ell} . \tag{A.3}$$

The first product on the r.h.s. of (A.3) is given by

$$\prod_{k=0}^{m-a-1} \left(n^2 \, 2^{-2k} \right)^{-2^k} = 2^4 n^2 \left[(4T_a)^{2/T_a} \right]^{-n} , \tag{A.4}$$

and the second product is evaluated for a large n as follows:

$$\begin{aligned} \prod_{\ell=0}^{m-a-1} \left(1 - n^{-2} 2^{2\ell} \right)^{-2^\ell} &= \exp \left(- \sum_{\ell=0}^{m-a-1} 2^\ell \ln \left(1 - n^{-2} 2^{2\ell} \right) \right) \\ &= \exp \left(\sum_{p=1}^{\infty} \frac{n^{-2p}}{p} \sum_{\ell=0}^{m-a-1} 2^{(1+2p)\ell} \right) \\ &= \exp \left(\sum_{p=1}^{\infty} \frac{n \, T_a^{-2p-1} - n^{-2p}}{p(2^{2p+1} - 1)} \right) \\ &= \exp \left(\frac{S_a}{T_a} n - \frac{1}{7} n^{-2} + \mathcal{O}(n^{-4}) \right) . \end{aligned} \tag{A.5}$$

Plugging (A.3) with (A.4) and (A.5) into (A.2) and rearranging other factors in (A.2), we get (4.16).

References

[1] A. Sen, *Rolling tachyon*, *J. High Energy Phys.* **04** (2002) 048 [hep-th/0203211].

[2] C.G. Callan Jr., I.R. Klebanov, A.W.W. Ludwig and J.M. Maldacena, *Exact solution of a boundary conformal field theory*, *Nucl. Phys.* **B 422** (1994) 417 [hep-th/9402113].

[3] J. Polchinski and L. Thorlacius, *Free fermion representation of a boundary conformal field theory*, *Phys. Rev.* **D 50** (1994) 622 [hep-th/9404008].

[4] A. Recknagel and V. Schomerus, *Boundary deformation theory and moduli spaces of D-branes*, *Nucl. Phys.* **B 545** (1999) 233 [hep-th/9811237].

[5] A. Sen, *Tachyon matter*, *J. High Energy Phys.* **07** (2002) 065 [hep-th/0203265].

[6] T. Okuda and S. Sugimoto, *Coupling of rolling tachyon to closed strings*, *Nucl. Phys.* **B 647** (2002) 101 [hep-th/0208196].

[7] A. Sen, *Time evolution in open string theory*, *J. High Energy Phys.* **10** (2002) 003 [hep-th/0207105].

[8] P. Mukhopadhyay and A. Sen, *Decay of unstable D-branes with electric field*, *J. High Energy Phys.* **11** (2002) 047 [hep-th/0208142].

[9] A. Sen, *Field theory of tachyon matter*, *Mod. Phys. Lett.* **A 17** (2002) 1797 [hep-th/0204143].

[10] A. Sen, *Time and tachyon*, hep-th/0209122.

[11] K. Hashimoto, P.-M. Ho and J.E. Wang, *S-brane actions*, *Phys. Rev. Lett.* **90** (2003) 141601 [hep-th/0211090].

[12] G. Gibbons, K. Hashimoto and P. Yi, *Tachyon condensates, carrollian contraction of Lorentz group and fundamental strings*, *J. High Energy Phys.* **09** (2002) 061 [hep-th/0209034].

[13] J.A. Minahan, *Rolling the tachyon in super BSFT*, *J. High Energy Phys.* **07** (2002) 030 [hep-th/0205098].

[14] S. Sugimoto and S. Terashima, *Tachyon matter in boundary string field theory*, *J. High Energy Phys.* **07** (2002) 025 [hep-th/0205085].

[15] K. Ohta and T. Yokono, *Gravitational approach to tachyon matter*, *Phys. Rev.* **D 66** (2002) 125009 [hep-th/0207004].

[16] B. Chen, M. Li and F.-L. Lin, *Gravitational radiation of rolling tachyon*, *J. High Energy Phys.* **11** (2002) 050 [hep-th/0209222].

[17] N. Lambert, H. Liu and J. Maldacena, *Closed strings from decaying D-branes*, hep-th/0303139.

[18] E. Witten, *Noncommutative geometry and string field theory*, *Nucl. Phys.* **B 268** (1986) 253.

[19] A. Sen and B. Zwiebach, *Large marginal deformations in string field theory*, *J. High Energy Phys.* **10** (2000) 009 [hep-th/0007153].

[20] N. Moeller and B. Zwiebach, *Dynamics with infinitely many time derivatives and rolling tachyons*, *J. High Energy Phys.* **10** (2002) 034 [hep-th/0207107].

[21] I.Y. Aref'eva, L.V. Joukovskaya and A.S. Koshelev, *Time evolution in superstring field theory on non-BPS brane. i: rolling tachyon and energy-momentum conservation*, hep-th/0301137.

[22] Y. Volovich, *Numerical study of nonlinear equations with infinite number of derivatives*, math-ph/0301028.

[23] N. Moeller, A. Sen and B. Zwiebach, *D-branes as tachyon lumps in string field theory*, *J. High Energy Phys.* **08** (2000) 039 [hep-th/0005036].

[24] K. Ohmori, *A review on tachyon condensation in open string field theories*, hep-th/0102085.

[25] H. Hata, *Quantization of nonlocal field theory and string field theory, 1*, *Phys. Lett.* **B 217** (1989) 438; *Quantization of nonlocal field theory and string field theory, 2*, *Phys. Lett.* **B 217** (1989) 445; *Brs invariance and unitarity in closed string field theory*, *Nucl. Phys.* **B 329** (1990) 698; *Construction of the quantum action for path integral quantization of string field theory*, *Nucl. Phys.* **B 339** (1990) 663.

[26] D.A. Eliezer and R.P. Woodard, *The problem of nonlocality in string theory*, *Nucl. Phys.* **B 325** (1989) 389.

[27] H.-t. Yang, *Stress tensors in p-adic string theory and truncated OSFT*, *J. High Energy Phys.* **11** (2002) 007 [hep-th/0209197].

[28] J. Kluson, *Time dependent solution in open bosonic string field theory*, hep-th/0208028.

[29] T. Takahashi and S. Tanimoto, *Wilson lines and classical solutions in cubic open string field theory*, *Prog. Theor. Phys.* **106** (2001) 863 [hep-th/0107046]; *Marginal and scalar solutions in cubic open string field theory*, *J. High Energy Phys.* **03** (2002) 033 [hep-th/0202133];
I. Kishimoto and T. Takahashi, *Open string field theory around universal solutions*, *Prog. Theor. Phys.* **108** (2002) 591 [hep-th/0205275];
T. Takahashi, *Tachyon condensation and universal solutions in string field theory*, hep-th/0302182.

[30] L. Rastelli, A. Sen and B. Zwiebach, *String field theory around the tachyon vacuum*, *Adv. Theor. Math. Phys.* **5** (2002) 353 [hep-th/0012251]; *Classical solutions in string field theory around the tachyon vacuum*, *Adv. Theor. Math. Phys.* **5** (2002) 393 [hep-th/0102112]; *Boundary CFT construction of D-branes in vacuum string field theory*, *J. High Energy Phys.* **11** (2001) 045 [hep-th/0105168];
D. Gaiotto, L. Rastelli, A. Sen and B. Zwiebach, *Ghost structure and closed strings in vacuum string field theory*, hep-th/0111129.

[31] H. Hata and T. Kawano, *Open string states around a classical solution in vacuum string field theory*, *J. High Energy Phys.* **11** (2001) 038 [hep-th/0108150];
H. Hata and S. Moriyama, *Observables as twist anomaly in vacuum string field theory*, *J. High Energy Phys.* **01** (2002) 042 [hep-th/0111034];
H. Hata, S. Moriyama and S. Teraguchi, *Exact results on twist anomaly*, *J. High Energy Phys.* **02** (2002) 036 [hep-th/0201177];
H. Hata and S. Moriyama, *Reexamining classical solution and tachyon mode in vacuum string field theory*, *Nucl. Phys.* **B 651** (2003) 3 [hep-th/0206208];
H. Hata and H. Kogetsu, *Higher level open string states from vacuum string field theory*, *J. High Energy Phys.* **09** (2002) 027 [hep-th/0208067].

[32] Y. Okawa, *Open string states and D-brane tension from vacuum string field theory*, *J. High Energy Phys.* **07** (2002) 003 [hep-th/0204012].